Available online at www.sciencedirect.com
ScienceDirect
Polymer 48 (2007) 348–355
polymer
www.elsevier.com/locate/polymer

Imaging of nonlinear optical response in biopolyesters via second harmonic generation microscopy and its dependence on the crystalline structures

Jun Xu [a,*], Jin Bao [b], Bao-Hua Guo [a], Hui Ma [b,c,**], Tian-Liang Yun [b], Liang Gao [b], Guo-Qiang Chen [d], Tadahisa Iwata [e]

[a] *Institute of Polymer Science and Engineering, Department of Chemical Engineering, Tsinghua University, Beijing 100084, China*
[b] *Department of Physics, Tsinghua University, Beijing 100084, China*
[c] *Graduate School at Shenzhen, Tsinghua University, Shenzhen 518055, China*
[d] *Department of Biological Sciences and Biotechnology, Tsinghua University, Beijing 100084, China*
[e] *Polymer Chemistry Laboratory, RIKEN Institute, Hirosawa, Wako-shi, Saitama 351-0198, Japan*

Received 21 July 2006; received in revised form 13 November 2006; accepted 16 November 2006
Available online 4 December 2006

Abstract

Nonlinear optical response in various polyhydroxyalkanoates (PHAs) was investigated via second harmonic generation microscopy (SHGM). It was revealed that the second harmonic generation (SHG) efficiency depended on both the polymer chemical structure and the crystalline structure. Among the PHAs studied, the microbial polyesters, poly(*R*-3-hydroxybutyrate) (PHB) and poly(*R*-3-hydroxyvalerate) (PHV) showed strongest SHG activity, which could be attributed to hydrogen bonding that enhanced hyperpolarizability of the carbonyl groups in the crystalline lamellar core, and the noncentrosymmetric arrangement of the SHG moieties. The β- and γ-type poly(β-propiolactone) demonstrated different SHG efficiency due to the different packing scheme of the chain stems in the crystal lattice despite the same chain conformation. In addition, SHG response in the banded spherulite varied with the lamellar orientation. Furthermore, SHGM was applied for 3-D imaging of PHB spherulite in PHB/poly(ε-caprolactone) blends via optical sectioning of the thick film at different depths. For PHB/poly(L-lactide) (PLLA) blends, SHGM revealed that the PHB twisting lamellae formed from the melt confined between the preformed PLLA twisting lamellae had the same twisting period as the latter, which could not be observed under polarized optical microscope. Due to the advantages, SHGM is expected to find more applications in characterization of nonlinear optical (NLO) materials with heterogeneous structures.

Keywords: Second harmonic generation microscopy; Polyhydroxyalkanoates; Crystalline structure

1. Introduction

Nonlinear optical (NLO) response has attracted extensive interest in the past decades, not only due to its potential applications in novel electro-optical devices but also due to its capability to reveal the structure and dynamic process of materials. Second harmonic generation (SHG) is a nonabsorptive frequency doubling of an excitation laser and has been observed in a wide variety of inorganic crystals [1], organic crystals [2] and NLO polymers [3]. It is of particular interest that SHG response has been reported in a variety of biological assemblies, such as collagen [4], microtubules, muscle myosin [5] and even cellulose [6]. The phenomenon has been utilized for imaging of biological tissues, living cells, and tumor in vivo [7–9]. It is reported that patho-physiological changes of the tissues, e.g. collagen, would lead to variation of the intensity and the polarization state of the observed SHG response

* Corresponding author. Tel./fax: +86 10 6278 4550.
** Corresponding author. Tel./fax: +86 755 26036238.
E-mail addresses: jun-xu@mail.tsinghua.edu.cn (J. Xu), mahui@tsinghua.edu.cn (H. Ma).

0032-3861/$ - see front matter © 2006 Elsevier Ltd. All rights reserved.
doi:10.1016/j.polymer.2006.11.037

[10,11]. Nevertheless, origin of the varied SHG response is still poorly understood due to the complicated hierarchical structures of the biological tissues. To solve the problem, it is necessary to investigate the effect of changes of different levels of structure on SHG using a model material system.

Polyhydroxyalkanoates are a family of biological polyesters with biodegradability and biocompatibility that may find applications in a variety of biomedical fields [12]. Recently, SHG activity was observed in the blends of two microbial polyesters, poly(3-hydroxybutyrate) (PHB) and poly(3-hydroxybutyrate-*co*-3-hydroxyhexanoate) (PHBHHx) [13]. This implies that normal semicrystalline PHA may possess NLO activity; however, little is known about the SHG mechanism. Previously, only the microbial PHAs with side chains containing NLO chromophores, such as cyanophenoxy group [14], were reported to demonstrate SHG activity. On the other hand, the semicrystalline PHAs possess hierarchical structures in their crystals, which is similar to biological assemblies but with tunable molecular and high-order structures. Consequently, they can be ideal model for investigation of the dependence of SHG behavior on various levels of structures. The study would be beneficial to understand SHG response in the biological assemblies.

Second harmonic generation microscopy (SHGM) is able to provide spatial distribution of SHG response in the material with resolution down to submicrons [15]. Hence, dependence of the SHG activity on the material structures of PHAs could be investigated. In this paper, for the first time, SHG behaviors in various PHAs were examined using SHGM. The potential of SHGM as a new tool for characterization of biomaterials with heterogeneous structures including crystalline/crystalline polymer blends was exploited.

2. Experimental section

2.1. Materials

PHAs with different monomer units were investigated. Poly(L-lactide) (PLLA) was purchased from Birmingham Polymers Inc., which has an inherent viscosity of 0.70 dL/g in 1 mg/mL chloroform at 30 °C. Poly(*R*-3-hydroxybutyrate) (PHB) with M_n 522,000 and M_w 775,000 was purchased from the Institute of Microbiology, Chinese Academy of Sciences. Poly(*R*-3-hydroxyvalerate) (PHV) with $M_w = 1{,}760{,}000$ and $M_w/M_n = 2.8$ was isolated from a recombinant *Ralstonia eutropha* harboring the PHA-biosynthesis genes of *Aeromonas caviae* [16]. Poly(β-propiolactone) (PPL) sample with $M_w = 367{,}000$ and $M_w/M_n = 2.2$ was kindly supplied by Tokuyama Corp. Poly(δ-valerolactone) (PVL) sample with $M_w = 62{,}000$ and $M_w/M_n = 1.8$ was synthesized by the ring-opening polymerization of δ-valerolactone (Tokyo Kasei Kogyo Co., Ltd.) with poly(methylaluminoxane) as a catalyst [17]. Poly(ε-caprolactone) (PCL) with $M_n = 10{,}000$ and $M_w/M_n = 1.4$ was purchased from Aldrich Chemicals and used without further purification. Poly(*R*-3-hydroxyoctanoate-*co*-*R*-3-hydroxydecanoate) (PHOD) with $M_n = 120{,}000$ and $M_w = 280{,}000$ is a random copolymer of *R*-3-hydroxyalkanoate with 6–14 carbon atoms with *R*-3-hydroxyoctanoate and *R*-3-hydroxydecanoate as major monomer units, which was synthesized by growing *Pseudomonas stutzeri* 1317 on glucose [18].

To reveal the sole effect of the degree of crystallinity on SHG activity, PHB blends with different content of a miscible amorphous polymer were prepared. PHB/atactic poly(D,L-lactide) (PDLLA) blends with blending ratio of 100/0, 80/20, 70/30, 60/40, 50/50, 40/60, 30/70 and 20/80 wt/wt, respectively, were cast from 1% chloroform solution.

To examine the effect of the thickness of the lamellar crystals and the degree of crystallinity on SHG activity, several PHB copolymers were utilized. Poly(3-hydroxybutyrate-*co*-10 mol% 3-hydroxyvalerate) (PHBV) from ICI was used as received. Poly(*R*-3-hydroxybutyrate-*co*-*R*-3-hydroxyhexanoate) (PHBHHx) random copolymers with 5 mol% HHx (P(3HB-*co*-5%-3HHx)) and 10 mol% HHx (P(3HB-*co*-10%-3HHx)) were synthesized by *Aeromonas hydrophila* 4AK4 and its recombinant strains [19].

All the samples sandwiched between two clean glass slides were melted on a hot stage at a temperature of 50 °C higher than the melting point. They were transferred to another stage with preset temperature to allow isothermal crystallization. After sufficient crystallization time depending on the crystallization rate, the melt-crystallized samples were slowly cooled down to room temperature and used for further structural characterizations.

2.2. Characterization

Polarized optical microscopy (POM) was applied to obtain the spherulitic morphology on a polarized optical microscope (BH-2, Olympus) coupled with a computer controlled CCD-camera (Sanyo Electric Co. Ltd.).

Differential scanning calorimetry (DSC) analysis was performed to study the thermal behavior of the melt-crystallized PHAs on a DSC-60 (Shimadzu) differential scanning calorimeter. The equipment was calibrated with indium standard and nitrogen atmosphere was used throughout the study. In the heat run, the specimens with weight around 2 mg sealed in an aluminum pan were heated from room temperature to 220 °C at a rate of 10 °C/min. From the endotherm on the curve, melting point and the fusion enthalpy were directly determined. The degree of crystallinity was obtained via dividing the fusion enthalpy of the tested sample by the reported value (146 J/g) of the 100% crystalline sample [20].

A two-photon fluorescence microscope (BioRad MRC1024 MP) was modified for second harmonic generation microscopy. The light source was a Ti:sapphire femto second laser system (Millennium V pumped Tsunami Lite, Spectra Physics), which provided ~120 fs polarized short pulses at 80 MHz rep rate and 810 nm wavelengths. The transmission imaging channel was replaced with a tailor-made detection arm to take forward propagating SHG. In each SHG channel, a 10 nm pass-band filter centered at 405 nm was used to filter through the narrow band SHG, and a high OD blocking filter was used to reject the 810 nm fundamental laser light.

3. Results and discussion

3.1. Dependence of SHG response on the structures of PHAs

SHG activity of the various semicrystalline PHAs was examined via SHGM. Though these polyesters were homologues in chemical structure, they exhibited sharp difference in the second-order nonlinear optical response (Table 1). Among them, PHB and PHV demonstrated the strongest SHG signal, while PLLA and PPL possessed very weak SHG. In contrast, PVL and PCL did not reveal observable SHG signal. For the first time, these normal polyesters containing only C, H and O atoms, were revealed to exhibit second harmonic generation.

All the amorphous samples of these polyesters did not reveal any observable SHG, which agrees with the general symmetry rule that electrodipole-induced SHG is forbidden in randomly disordered media [21]. Therefore, it is obvious that the SHG activity in the semicrystalline PHAs originates from the crystalline structure. To investigate the effect of degree of crystallinity (X_c), PHB/amorphous atactic-PLA (PDLLA) blends with various blending ratios were prepared via crystallization at 90 °C. X_c in the whole sample varied in a wide range depending on the blending ratio. SHG intensity is proportional to X_c^2 (Fig. 1).

SHG response of the PHB copolymers was investigated as well. Incorporation of a second comonomer into PHB led to decrease of X_c and SHG intensity (Table 2). In terms of the crystalline structure, copolymerization resulted in decrease of both X_c and the thickness of the lamellar core. Via normalization of the measured SHG intensity to X_c^2, the effect of lamellar thickness could be deduced. The normalized SHG efficiency increased slightly with decease of the lamellar core thickness (Table 2). The reason is still not clear.

Table 1
SHG activity of different types of polyhydroxyalkanoates with urea as a standard

Sample	PLLA	PHB	PHV	PPL	PVL	PCL	PHOD	Urea
SHG intensity (arbitrary)	2.8	8200	810	11	0	0	0	12,000

PLLA, poly(L-lactide); PHB, poly(*R*-3-hydroxybutyrate); PHV, poly(*R*-3-hydroxyvalerate); PPL, poly(β-propiolactone); PVL, poly(δ-valerolactone); PCL, poly(ε-caprolactone); PHOD, poly(*R*-3-hydroxyoctanoate-*co*-*R*-3-hydroxydecanoate).

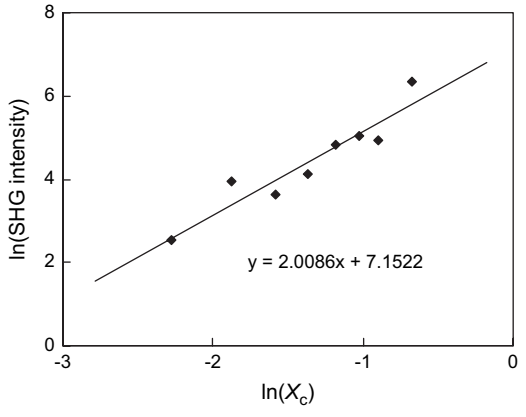

Fig. 1. Dependence of SHG intensity in PHB/atactic-PLA blends on the degree of crystallinity (X_c).

Table 2
SHG activity of PHB copolymers

Sample	X_c (%)	SHG intensity (a.u.)	Normalized SHG (a.u.)
PHB	47	91	412
PHBV	36	42	324
P(HB-*co*-5%HHx)	30	45	500
P(HB-*co*-10%HHx)	15	15	667

Normalized SHG was calculated by dividing SHG intensity by X_c^2.

According to the theory of SHGM [15,22], SHG signal intensity scales as

$$I_{SHG} \propto \left[\frac{N_S\langle\beta\rangle P}{\tau}\right]^2 \tau \quad (1)$$

where N_S is the density of SHG moiety, P is the laser pulse energy, τ is the laser pulse width, and $\langle\beta\rangle$ denotes an orientation averaged hyperpolarizability. According to the theoretical prediction, the intensity of SHG varies quadratically with the density of the SHG moiety. From the experimental result that SHG intensity is proportional to X_c^2, we conclude that the crystalline core of the PHA lamellae contributes to the SHG response.

Eq. (1) also shows that SHG intensity depends on both the hyperpolarizability β of the dipole (the molecular property) and its spatial distribution, a property relevant to the structures of the condensed state.

Usually, SHG activity results from the conjugated groups in NLO polymers, so we can suggest that SHG in PHAs is due to the carbonyl groups. Though the concerned PHAs are a family of homologues in chemical structure, the hyperpolarizability probably varies from one to another, which is supported by the fact that in some NLO materials, e.g. urea and other organic crystals, hydrogen bonding enhances the hyperpolarizability and thus the final SHG efficiency [23–25]. It has been reported that C–H···O hydrogen bonds exist between the C=O group and the CH_3 group in the crystallized PHB and its copolymers, reflected from shifting of ν(C=O) from 1748 cm^{-1} in the melt to 1724 cm^{-1} in the crystallized film on the FTIR spectrum [26,27]. Amplitude of the peak shift of ν(C=O) can reflect the relative strength of the hydrogen bonds (Fig. 2). Among the PHAs studied, PHB and PHV showed maximal peak shift, PPL ranked next, while PLA and PVL hardly revealed any peak shift of ν(C=O). The order of peak shift agrees with the order of SHG intensity, therefore, it is proposed that hydrogen bonding probably plays an important role in the

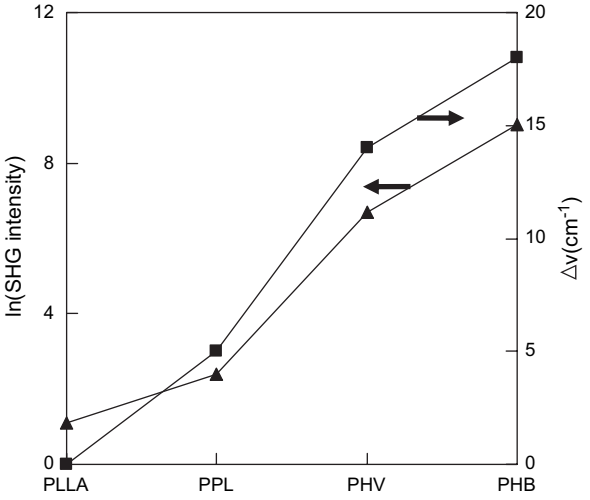

Fig. 2. SHG efficiency related to hydrogen-bonding strength in the crystallized PHAs. $\Delta\nu$ denotes the shifting of C=O stretching vibration during crystallization, reflected from the IR spectra.

strong SHG efficiency of PHB and PHV observed in this study.

On the other hand, the SHG intensity varied with the orientation averaged hyperpolarizability $\langle\beta\rangle$. In the amorphous PHAs, centrosymmetric packing of the dipoles resulted in a zero value of $\langle\beta\rangle$, as a result, SHG response was not observed. Among the PHAs, PLA, PHB, PHV are enantiomeric polymers, which enable noncentrosymmetric packing of the ester groups, while in the crystallized PCL the dipoles of the racemic polymer adopt antiparallel orientation in neighboring chain stems, leading to cancelled SHG activity. This is also the case for the even-number nylons. Though there exists strong N–H···O hydrogen bonds, they are packed in a centrosymmetric manner [28], resulting in zero $\langle\beta\rangle$. This is the reason why we did not observe SHG response in the crystallized nylon 6 and nylon 66. In the β- and γ-modification of PPL crystals, despite the same all-*trans* conformation of the chain stems, the C=O dipoles adopt different arrangement in the crystalline lattice. In the β-PPL the dipoles are oriented in the antiparallel directions in neighboring layers, while in the γ-PPL they are arranged in the two perpendicular directions [29]. Therefore, SHG activity was observed in the γ-modification of PPL crystals but not in the β-modification (Fig. 3a and b).

During the melt crystallization process, PHB, PHV and their copolymers formed banded spherulites [20,30,31] with alternative bright and dark bands observed between crossed polarizers under a linear optical microscope (Fig. 4a). When the banded spherulites were observed via SHGM, they also exhibited alternative bright and dark bands (Fig. 4b) with the same spacing as that observed under the linear optical microscope. Previous AFM [32–34] and microfocus WAXD [35,36] studies confirmed that the bands resulted from lamellar twisting. In the edge-on lamellae, the chain stems run parallel to the substrate; while in the flat-on lamellae, chain stems pointed normal to the substrate. Similar to the linear optical microscopy, the brighter domain in the SHG micrograph indicates the stronger SHG intensity (Fig. 4b). Apparently, the varied SHG intensity in these bands resulted from the different orientation of chain stems.

Systematic study on the effect of other factors, such as the chain conformation and orientation order of the lamellae is still in progress. Nevertheless, the preliminary results reported here unambiguously demonstrate the dependence of the SHG intensity on both the chemical structures and the condensed state. Thus, SHGM provides a novel method to distinguish different types of PHAs. In addition, since the amorphous PHAs do not exhibit any SHG activity, SHG imaging will be suitable to study the in vivo state of the granules of PHB or its copolymers.

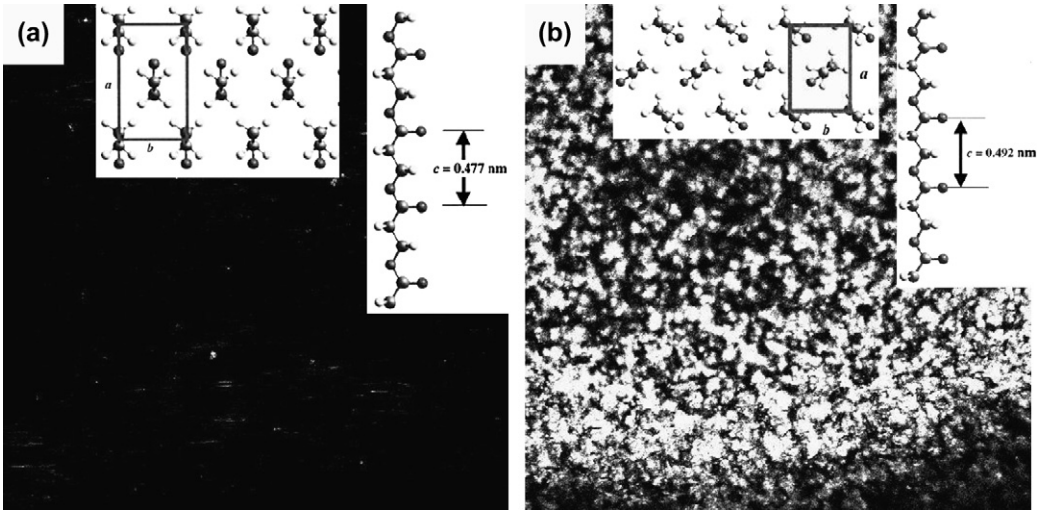

Fig. 3. SHG response of different crystalline modifications of poly(β-propiolactone) (PPL): (a) β-type PPL obtained from heat drawing of the solution cast film; (b) γ-type PPL cast from chloroform solution. Inset shows the packing scheme of the chain segments in the crystal lattice, which is adopted from Ref. [16].

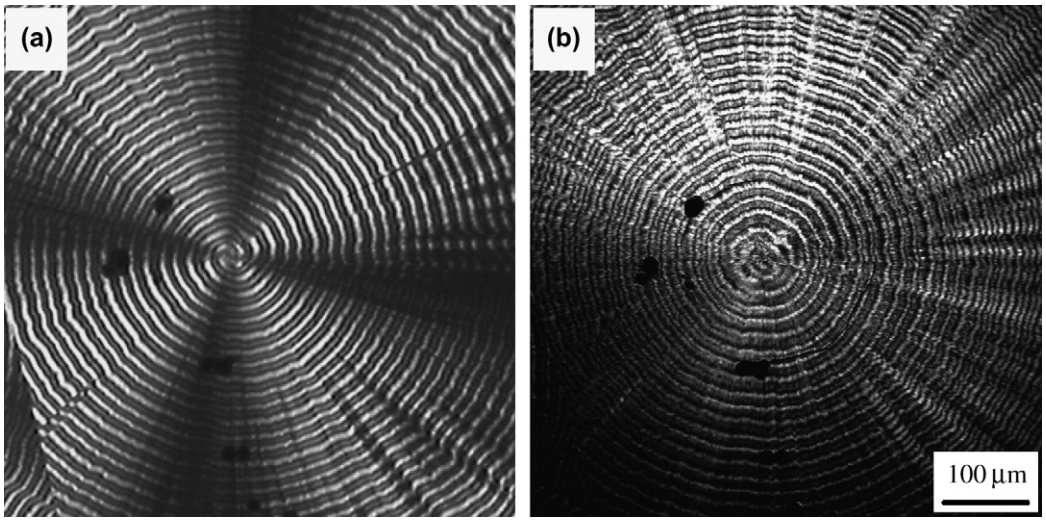

Fig. 4. The banded spherulite of poly(*R*-3-hydroxybutyrate-*co*-5 mol% *R*-3-hydroxyhexanoate) observed under (a) polarized linear optical microscope; (b) SHG microscope.

3.2. Applications of second harmonic generation microscopy

Selective and nondestructive three-dimensional imaging of one component in a thick film of the crystalline/crystalline polymer blends with similar chemical structure has been an unresolved problem. Taking a 300-μm-thick immiscible poly(*R*-3-hydroxybutyrate) (PHB)/poly(ε-caprolactone) (PCL) blend film as an example, the weak difference in the refractive indices of the two components and the high scattering nature of the opaque blends make it hard for linear optical microscopy to obtain the spatial distribution of any component. Nevertheless, in the blends, PHB shows strong SHG while PCL is SHG-inactive; as a result, SHGM is expected to fulfill the task. Compared with the normal linear optical microscopy, SHGM demonstrates additional advantages for imaging a thick sample: 3-D images can be obtained via optical sectioning in different depths. In addition, compared with the fluorescence confocal microscopy, SHGM does not require staining of the sample by additional fluorescent probes, consequently, SHGM will not perturb the materials. At a PHB/PCL blending ratio of 30/70 (wt/wt), PHB formed the dispersed phase in the continuous PCL matrix. After melted at 200 °C, the blend was first maintained at 90 °C (higher than the T_m of PCL) to turn PHB fully crystallize while PCL remained amorphous. Due to the low nucleation density of PHB, only one spherulite was formed in each drop of PHB melt. After complete crystallization of PHB, the blend film was quenched to room temperature to allow PCL crystallization. The morphology of a PHB spherulite dispersed in PCL matrix is clearly observable (Fig. 5), where the bright region shows an SHG-active PHB spherulite and the dark region consists of SHG-negative PCL spherulites. The primary nucleus of the PHB spherulite formed at the PHB/PCL interface is well visible (Fig. 5d).

In addition, SHGM can be applied to selectively image one component in miscible crystalline/crystalline PHA blends, for example, to selectively image PHB lamellae sandwiched between PLLA lamellae. Since PHB and PLLA are miscible in the melt, after crystallization they form complicated morphology in the spatial distribution of the two components. It was reported that PLLA could form banded spherulites when crystallized from its melting state [37]. When the PHB/PLLA 50/50 blend melt was maintained at 130 °C for 12 h, PLLA formed banded spherulite while PHB still remained amorphous in the interlamellar region of PLLA. Then the blend was quenched to 90 °C, allowing PHB crystallization. The preformed twisting PLLA lamellae provided physical confinement for the growth of PHB lamellae.

In an attempt to observe whether the previously formed twisting PLLA lamellae could affect the twisting of PHB lamellae grown from the confined melt, the following studies were performed: PLLA formed banded spherulites with lamellar twisting period about 75 μm when it was maintained at 130 °C [37], while bulk PHB formed banded spherulites with a narrower twisting period around 15 μm when it was maintained at 90 °C [38]. Due to the multilayered sandwich structure, polarized optical microscopy could not distinguish PHB from PLLA (Fig. 6a). Nevertheless, SHGM can easily fulfill the challenging task because PHB shows much stronger SHG than PLLA does. When laser power was reduced to certain content, only PHB was observable in the film. Selective imaging of the sandwiched PHB lamellae revealed that the confined PHB lamellae twisted with a period of 75 μm, the same as the preformed PLLA lamellae (Fig. 6b). Consequently, SHGM confirms that the preformed twisting PLLA lamellae did act as the growth templates of PHB lamellae.

Furthermore, SHGM can be used to determine the absolute orientation, symmetry and the degree of orientation order of the molecules in each microdomain via polarization anisotropy [39,40]. As a result, SHGM has been extensively used for imaging of the high-order biological structures; however, it has rarely been adopted for characterization of NLO polymers, except for a few recent reports [41,42]. It is expected that SHGM will find wide applications in characterization of NLO polymer materials.

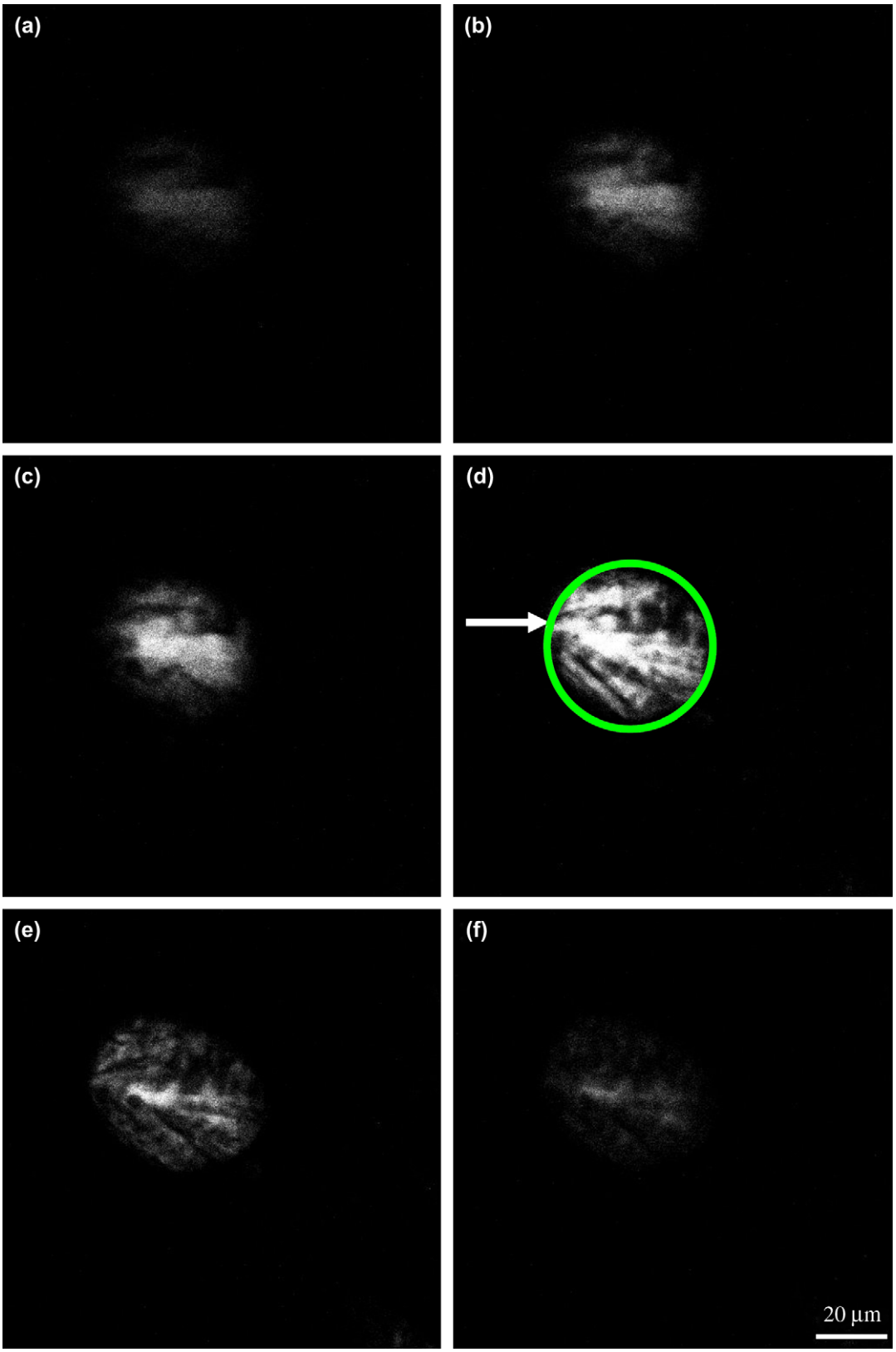

Fig. 5. 3-D SHG images of a PHB spherulite formed in PCL matrix. The images were acquired via optical sectioning every 15 μm in depth. The circle indicates the spherical interface between PHB and PCL. Head of the white arrow points to the primary nucleus at the interface of the two components.

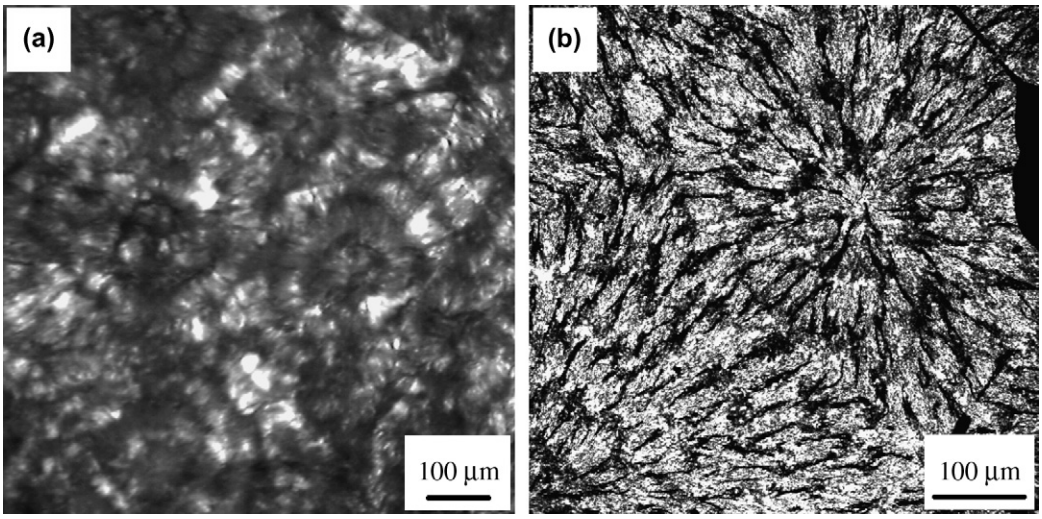

Fig. 6. Microscopic images of PLLA/PHB blends in which PHB lamellae were crystallized from the melt confined between twisting PLLA lamellae. (a) Polarized optical microscopy revealing both PLLA and PHB morphology, in which each component could not be distinguished; (b) second harmonic imaging microscopy, which reveals only the morphology of PHB.

4. Conclusion

It is shown that a variety of semicrystalline PHAs possessed SHG activity, which varied considerably among the examined polymers. Among them, PHB and PHV exhibited the strongest SHG intensity, which was attributed to the C–H···O hydrogen bonds between the C=O groups and the CH_3 groups and the noncentrosymmetric packing of the dipoles in the crystalline lattice. SHG response varied quadratically with the degree of crystallinity in PHB blends and copolymers. Consequently, the SHG activity results from the crystalline core of the lamellae. The β- and γ-type poly(β-propiolactone) demonstrated varied SHG efficiency due to the different packing scheme of the chain stems in the crystalline lattice despite the same chain conformation. Lamellar twisting in the banded spherulites of microbial PHAs led to periodical alteration of SHG intensity along the spherulite radius. Dependence of SHG response on both the chemical structure and the condensed state enables SHGM to find applications in characterization of PHA materials with heterogeneous structure. The 3-D morphology of a PHB spherulite in PHB/PCL blend film with thickness up to hundreds of microns was nondestructively imaged via optical sectioning function of SHGM. Furthermore, PHB lamellae crystallized from the melt confined between twisting PLLA lamellae in PLLA/PHB blends were also observed under SHGM, which could not be distinguished under polarized optical microscope. When grown from the confined melt sandwiched between twisting PLLA lamellae, the PHB lamellae showed the same twisting period as the preformed PLLA lamellae, which confirmed the template effect of the latter.

Acknowledgments

We are grateful for the financial support from Tsinghua Basic Research Foundation (Grant No. Jc2003037), the National Natural Science Foundation of China (Grant Nos. 20334020, 60138010, 20504019) and the state "863" high-tech project (Grant No. 2002AA213051).

References

[1] Hellwarth R, Christensen P. Opt Commun 1974;12:318–22.
[2] Ohkita M, Suzuki T, Nakatani K, Tsuji T. Chem Commun 2001;(16): 1454–5.
[3] Kajzar F, Lee KS, Jen AKY. Adv Polym Sci 2003;161:1–85.
[4] Freund I, Deutsch M, Sprecher A. Biophys J 1986;50:693–712.
[5] Both M, Vogel M, Fink RHA, Uttenweiler D. Proc SPIE 2003;5139: 112–20.
[6] Brown RM, Millard AC, Campagnola PJ. Opt Lett 2003;28:2207–9.
[7] Guo Y, Savage HE, Liu F, Schantz SP, Ho PP, Alfano PR. Proc Natl Acad Sci USA 1999;96:10854–6.
[8] Campagnola PJ, Loew LM. Nat Biotechnol 2003;21:1356–60.
[9] Brown E, McKee T, di Tomaso E, Pluen A, Seed B, Boucher Y, et al. Nat Med 2003;9:796–800.
[10] Kim BM, Eichler J, Reiser KM, Rubenchik AM, Da Silva LB. Laser Surg Med 2000;27:329–35.
[11] Lin XS, Pan L, Hu JY, Ma H, Chen DY. Prog Biochem Biophys 2004;31: 83–8 [Chinese].
[12] Sudesh K, Abe H, Doi Y. Prog Polym Sci 2000;25:1503–55.
[13] Deng Y, Lin XS, Zheng Z, Deng JG, Chen JC, Ma H, et al. Biomaterials 2003;24:4273–81.
[14] Gross RA, Kim O, Rutherford DR, Newmark RA. Polym Int 1996;39: 205–13.
[15] Campagnola PJ, Clark HA, Mohler WA, Lewis A, Loew LM. J Biomed Opt 2001;6:277–86.
[16] Fukui T, Kichise T, Yoshida Y, Doi Y. Biotechnol Lett 1997;19:1093–7.
[17] Furuhashi Y, Sikorski P, Atkins E, Iwata T, Doi Y. J Polym Sci Part B Polym Phys 2001;39:2622–34.
[18] Chen GQ, Xu J, Wu Q, Zhang ZM, Ho KP. React Funct Polym 2001;48: 107–12.
[19] Qiu YZ, Ouyang SP, Shen ZY, Wu Q, Chen GQ. Macromol Biosci 2004; 4:255–61.
[20] Barham PJ, Keller A, Otun EL, Holmes PA. J Mater Sci 1984;19: 2781–94.
[21] Kleinman DA. Phys Rev 1962;128:1761–75.
[22] Both M, Vogel M, Friedrich O, von Wegner F, Künsting T, Fink RHA, et al. J Biomed Opt 2004;9:882–92.
[23] Sarma JARP, Rao JL, Bhanuprakash K. Chem Mater 1995;7:1843–8.

[24] Wu KC, Snijders JG, Lin CS. J Phys Chem B 2002;106:8954–8.
[25] Skwara B, Gora RW, Bartkowiak W. Chem Phys Lett 2005;406:29–37.
[26] Xu J, Guo BH, Yang R, Wu Q, Chen GQ, Zhang ZM. Polymer 2002;43: 6893–9.
[27] Sato H, Murakami R, Padermshoke A, Hirose F, Senda K, Noda I, et al. Macromolecules 2004;37:7203–13.
[28] Atkins EDT, Hill MJ, Jones NA, Cooper SJ. J Polym Sci Part B Polym Phys 1998;36:2401–12.
[29] Furuhashi Y, Iwata T, Sikorski P, Atkins E, Doi Y. Macromolecules 2000; 33:9423–31.
[30] Saracovan I, Cox JK, Revol JF, Manley RSJ, Brown GR. Macromolecules 1999;32:717–25.
[31] Xu J, Guo BH, Chen GQ, Zhang ZM. Polym J 2003;35:460–4.
[32] Hobbs JK, Mcmaster TJ, Miles MJ, Barham PJ. Polymer 1998;39: 2437–46.
[33] Jiang Y, Zhou JJ, Li L, Xu J, Guo BH, Zhang ZM, et al. Langmuir 2003; 19:7417–22.
[34] Xu J, Guo BH, Zhang ZM, Zhou JJ, Jiang Y, Yan SK, et al. Macromolecules 2004;37:4118–23.
[35] Gazzano M, Focarete ML, Riekel C, Scandola M. Biomacromolecules 2000;1:604–8.
[36] Tanaka T, Fujita M, Takeuchi A, Suzuki Y, Uesugi K, Doi Y, et al. Polymer 2005;46:5673–9.
[37] Xu J, Guo BH, Zhou JJ, Li L, Wu J, Kowalczuk M. Polymer 2005;46: 9176–85.
[38] Xu J, Guo BH, Chen GQ, Zhang ZM. J Polym Sci Part B Polym Phys 2003;41:2128–34.
[39] Flörsheimer M, Bootsmann MT, Fuchs H. Adv Mater 2000;12: 1918–21.
[40] Mohler W, Millard AC, Campagnola PJ. Methods 2003;29:97–109.
[41] Martin G, Toussaere E, Soulier L, Zyss J. Synth Met 2002;127: 49–52.
[42] Lagugné-Labarthet F, Sourisseau C, Schaller RD, Saykally RJ, Rochon P. J Phys Chem B 2004;108:17059–68.